Modular synthesis and facile network formation of catechol functionalized triblock copolymers†

Fahed Albreiki, [a] Tobias Göckler [ab] and Samanvaya Srivastava *[acde]

We report the synthesis of catechol-functionalized symmetric triblock polymers comprising densely functionalized catechol endblocks using anionic ring-opening polymerization (AROP) and thiol–ene click chemistry. The simplicity and modularity of our approach rely on a two-step synthesis that eliminates the need for catechol protection and enables the functionalization of precisely synthesized precursor polymers with catechol-containing thiols. Partial oxidation of the catechols on the triblock polymers to quinones enabled rapid gelation (within seconds) while retaining strong adhesive attributes.

Polymers that establish strong surface-independent adhesion in aqueous environments are attractive materials in biomedical and industrial applications.[1] Mimicking the adhesive chemistry harnessed by marine organisms (*e.g.*, *Mytilus californianus* or California mussel, which secrete proteinaceous glues) has emerged as a versatile approach to achieve robust wet adhesion.[2,3] Interchain crosslinking and polymer–substrate anchoring of these protein glues is primarily attributed to 3,4-dihydroxyphenylalanine (DOPA) residue,[2 4] which can undergo covalent crosslinking through oxidative conversion of its catechol groups to quinone and subsequent catechol–quinone coupling.[3,5] At the same time, catechol groups form interfacial bonds with various surfaces through covalent bonds (Michael addition and Schiff base reactions) and non-covalent interactions (*e.g.*, hydrogen bonding and metal coordination).[6 8] Hence, the incorporation of DOPA moieties in synthetic or bioderived polymers has been pursued to create adhesives and antifoulants[9 12] that can replace water molecules on wet substrates to achieve robust contact and adhesive bond formation through diverse modalities.

Despite the widespread adoption of catechol adhesion in synthetic platforms (for example, polypeptides,[9,13] polyamides,[14] and polyethylene glycol or PEG[5,11]), the adhesive properties of catechol adhesives are limited by the inability to tune the content and placement of catechol groups on the polymer backbones. The biocompatibility, hydrophilicity, and diversity of its end-group chemistries have made PEG an attractive candidate for facile catechol modification.[5,11,15] Linear and multi-arm PEG chains functionalized with catechol end groups have been demonstrated to form hydrogels through partial oxidation of the catechol chain ends (elastic modulus, $G' \sim 13$ kPa).[5] However, the oxidative conversion of singular catechol into quinone often compromises the network's interfacial binding affinity (lap shear adhesion strength ≤ 10 kPa on tissue[16]), leading to adhesion/cohesion trade-offs.[5,16] Furthermore, the phenolic coupling efficiency and the curing time through catechol–quinone bonding depends on the catechol redox potential and the intermediate conversion of DOPA into derivatives, resulting in polymers with singular DOPA end groups curing very slowly (hours to days).[5,16]

In this contribution, we report a modular strategy to synthesize catechol-functionalized PEG-based triblock polymers comprising densely functionalized catechol endblocks by utilizing anionic ring-opening polymerization (AROP) and thiol–ene click coupling chemistry (Scheme 1). While catechol-functionalized block and random copolymers have been synthesized,[17,18] catechol protection/deprotection steps were necessary to avoid undesirable oxidation of the catechol groups during synthesis. A key advantage in our approach is the highly efficient conversion of a widely available reagent, dopamine **1**, to DOPA-thiol **2**, which was amenable to thiol–ene click coupling under ultraviolet (UV) irradiation without the need for protection of catechol groups against oxidation. DOPA-thiol synthesis was achieved by aminolysis of thiolactones (namely γ-thiobutyrolactone), which can be efficiently ring-opened *via* nucleophilic amine groups in dopamine **1** to release thiols through a one-pot synthesis[19,20]

[a] *Department of Chemical and Biomolecular Engineering, University of California, Los Angeles, Los Angeles, CA 90095, USA. E-mail: samsri@ucla.edu*
[b] *Institute of Functional Interfaces, Karlsruhe Institute of Technology (KIT), 76344 Eggenstein- Leopoldshafen, Germany*
[c] *California NanoSystems Institute, University of California, Los Angeles, Los Angeles, CA 90095, USA*
[d] *BioPACIFIC MIP, University of California, Los Angeles, Los Angeles, CA 90095, USA*
[e] *Institute for Carbon Management, University of California, Los Angeles, Los Angeles, CA 90095, USA*

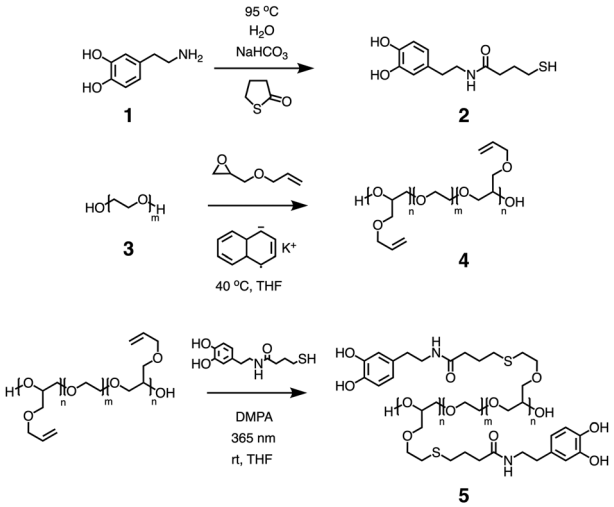

Scheme 1 Synthesis of catechol-functionalized triblock copolymers.

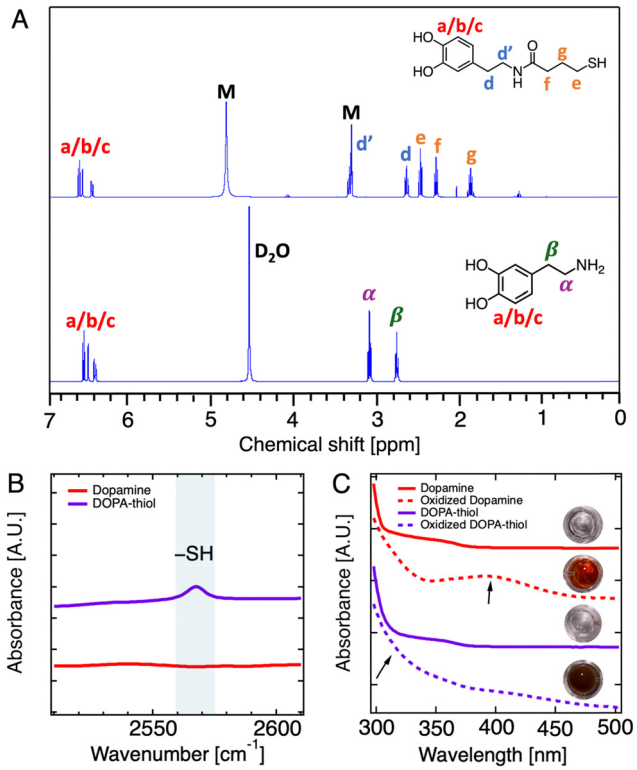

Fig. 1 Chemical analysis of dopamine 1 and DOPA-thiol 2. (A) ^{1}H NMR (letter M indicates deuterated methanol), (B) FTIR, and (C) UV-vis absorbance spectra. Photos of the corresponding samples are also shown in (C).

without exposing catechol groups to conditions that can result in their oxidation.

Symmetric ABA triblock polymer precursors were synthesized by oxy-anionic ring-opening polymerization of allyl glycidyl ether (AGE) from a PEG macroinitiator **3** to produce poly(allyl glycidyl ether-*block*-ethylene glycol-*block*-allyl glycidyl ether) (P(AGE-*b*-EG-*b*-AGE)) **4**, as shown in Scheme 1. The use of AGE as a monomer is advantageous because the controlled cyclic ring-opening of its epoxide groups enables the synthesis of symmetric triblock polymers with well-defined lengths and sequences and narrow length distributions while featuring a high density of reactive alkene functional groups on the endblocks. The terminal alkene groups along the PAGE backbone favor post-polymerization modification of endblocks through thiol–ene coupling.[21,22] Thus, DOPA-thiol reaction with terminal carbon–carbon double bonds can be pursued to create catechol-functionalized water-soluble symmetric triblock polymers **5** (referred to here as triblock polycatechol or tbPC).

The successful synthesis of the "clickable" DOPA-thiol **2** was confirmed *via* ^{1}H NMR and FTIR spectroscopy. Fig. 1A shows a ^{1}H NMR spectrum of DOPA-thiol **2**, contrasted against the spectrum of dopamine **1** (starting reagent). The successful formation of DOPA-thiol was signified by the peaks at chemical shifts δ = 1.81, 2.43, and 2.60 ppm while retaining the signatures of the catechol groups at δ = 6.50–6.66 ppm. Fourier-transform infrared (FTIR) spectra, shown in Fig. 1B, further corroborated the successful synthesis and highlighted the noticeable appearance of thiol stretching from **2** in the wavenumber range of 2550–2600 cm $^{-1}$, which was absent in **1**. Consonant chemical fingerprints between **1** and **2** were captured (Fig. S1A, ESI†), albeit with higher absorbances at wavenumbers corresponding to carbonyl (Fig. S1B, ESI†) and secondary amine (Fig. S1C and D, ESI†) attributable to **2**.

To confirm the absence of unwanted oxidation in **1** and **2**, the ultraviolet/visible (UV-vis) absorbance spectra of both species, shown as solid lines in Fig. 1C, were compared to their states after oxidation with sodium periodate ($NaIO_4$) (dashed lines). The unoxidized samples (39.5 mM of **1** and 29.5 mM of **2**) were transparent, showing nearly identical spectra with no peaks corresponding to the oxidized derivatives like quinone (which would appear at wavelength $\lambda \approx 400$ nm). Adding $NaIO_4$ (0.9 mM) to the dopamine **1** solution resulted in the appearance of brown color in the solution. Correspondingly, a broad absorbance peak with a maximum at $\lambda_{max} \approx 400$ nm, indicating quinone formation, appeared in the UV-Vis spectra. Similarly, DOPA-thiol **2** turned dark brown after adding $NaIO_4$, and increased absorbance at a wavelength approaching $\lambda \approx 300$ nm was observed. ^{1}H NMR analysis of the benzene rings in **1** and **2** also corroborated that catechol remained unchanged (Fig. 1A), unlike oxidized dopamine, which exhibited the spectra of oxidized DOPA derivatives (see Fig. S2, ESI†).

The successful synthesis and functionalization of symmetric triblock copolymers are demonstrated in Fig. 2, which contrasts the ^{1}H NMR spectra of the starting PEG midblock **3**, precursor polymer P(AGE-*b*-EG-*b*-AGE) **4**, and the functionalized product tbPC **5**. In Fig. 2A, only the methyl protons appear in the NMR spectra. The appearance of allyl protons from repeating AGE units (δ = 5.29 and 5.89 ppm) in Fig. 2B confirmed the growth of the PAGE blocks. Comparing the integrations of the allyl peaks of PAGE with the methylene peaks of PEG and PAGE (δ = 3.50–3.70 ppm) allowed estimation of the degree of polymerization of the PAGE blocks – estimated here to be n = 6. Gel permeation chromatograms, shown in Fig. 2D, confirmed (i) $m \approx 120$ and (ii) the growth of the PAGE blocks resulting in a noticeable

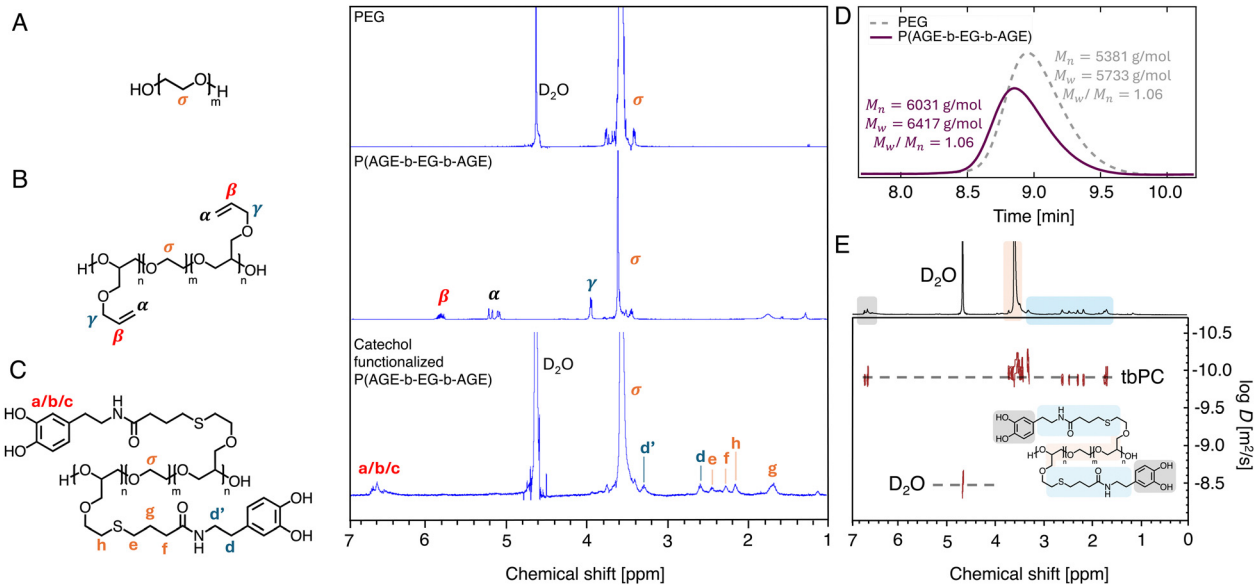

Fig. 2 ^{1}H NMR spectra of (A) PEG **3**, (B) triblock polymer (P(AGE-*b*-EG-*b*-AGE)) **4**, and (C) tbPC polymer **5**. (D) GPC chromatograms of PEG **3** and triblock polymer (P(AGE-*b*-EG-*b*-AGE)) **4**. (E) DOSY ^{1}H NMR spectra of tbPC polymer dissolved in D_2O at 298 K.

increase in M_W and M_n after AROP, indicated by the shift in retention times to lower values. Notably, the chain length distribution (M_W/M_n = 1.06) remained nearly unchanged after triblock synthesis, indicating products with very narrow molecular weight distributions.

Post-synthesis functionalization of PEG-based triblock polymers (as shown in Scheme 1) was pursued by utilizing thiol–ene click chemistry due to its mild reaction conditions at room temperature and quantitative yields.[23] Complete consumption of the allyl groups and the appearance of catechol peaks (δ = 6.50, 6.64, and 6.66 ppm) in Fig. 2C were observed, confirming the successful functionalization. DOSY spectra, shown in Fig. 2E, revealed that the PEG midblock and catechol functionalized endblocks have nearly the same diffusion coefficients, suggesting their presence on the same macromolecule. Moreover, their diffusion coefficients were ~30× smaller than that of the solvent (D_2O), pointing towards the large size of the tbPC macromolecule. FTIR spectroscopy contrasting **4** and **5** highlighted the appearance of carbonyl and an increase in hydroxyl stretch in **5**, likely due to the presence of catechol groups (see Fig. S3, ESI†). The resulting tbPC **5** was a densely functionalized, symmetric triblock polymer with catecholic endblocks and a PEG midblock.

The precise placement of catechol groups on the endblocks and their higher content (compared to a single terminal catechol group on a polymer chain) ameliorates the curing of catechol-based hydrogels and adhesives. We explored the hydrogelation of tbPC by characterizing their time-dependent oxidative crosslinking *via* torsional rheometry (Fig. 3). The curing of hydrogels based on our polymers was pursued *via* partial oxidation of their catechol units and catechol–quinone crosslinking, resulting in rapid hydrogelation and the formation of networks with high shear strengths. As representative systems,

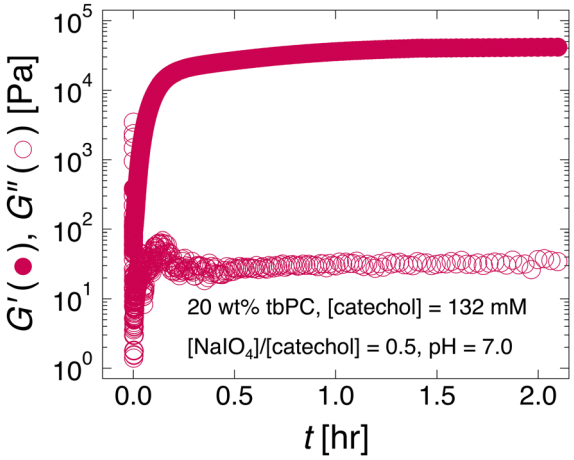

Fig. 3 Gelation of a tbPC hydrogel is tracked by monitoring the evolution of storage G' and loss G'' moduli.

20 wt% tbPC ([catechol] = 132 mM, pH = 7.0) was mixed with $NaIO_4$ to produce hydrogels with [$NaIO_4$]/[catechol] = 0.5. Instant changes in color and flow behavior were observed after $NaIO_4$ addition – suggesting the presence of oxidative polymerizations, which resulted in cross-linking between the catechol units.[5] The abrupt increase in elastic and loss moduli (G' and G''), shown in Fig. 3, indicated swift gelation. This fast gelation was possibly due to the abundance and variety of oxidized DOPA derivatives that increased the availability of cross-linkable groups and accelerated gelation. Within a few minutes, the storage modulus reached more than 10 kPa, and, in a little over an hour, plateaued at $G' \approx 45$ kPa.

Adhesion experiments on glass and collagen demonstrated diverse and robust adhesive attributes of tbPC hydrogels. The polymers were oxidized (10 wt%, [$NaIO_4$]/[catechol] = 0.5) and

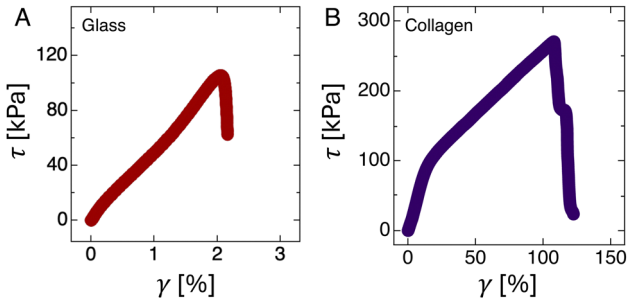

Fig. 4 Stress τ *versus* strain γ results from lap shear tests probing the adhesion strength of tbPC polymers on (A) glass and (B) collagen substrates.

allowed to cure between two substrate surfaces (a schematic of adhesive joint preparation is shown in Fig. S4, ESI†). The stress τ–strain γ relation obtained from lap shear adhesion tests is shown in Fig. 4A and B for glass and collagen substrates, respectively. A maximum lap shear strength $\tau_{max} \approx 0.1$ MPa with failure at $\gamma_{max} \approx 2\%$ was recorded when adhering to glass (Fig. 4A), ascribed to the hydrogen bonding between silanol groups on glass and the hydroxyl groups of catechol.[6] The adhesion on collagen exhibited $\tau_{max} \approx 0.3$ MPa and $\gamma_{max} \approx 100\%$ (Fig. 4B), likely arising from the covalent bonds between catechols and the quinones of the polymers and amine groups on collagen.[7,8] The higher γ_{max} observed during collagen stretching can be attributed to the extensible nature of collagen substrates.

In conclusion, we demonstrate a modular strategy to synthesize PEG-based triblock copolymers with controlled placement and content of catechol groups. This strategy eliminated the need for protection/deprotection steps of catechol by utilizing efficient ring opening of thiolactones to create catechol-containing monomers that are amenable to thiol–ene click chemistry. We further demonstrated the superiority of the catechol-containing triblock polymers in forming strong, adhesive hydrogels. We envisage the utility of this platform in creating hydrogel adhesive libraries with precisely tuned catechol functionality, sequence, and oxidation states.

S. S. and F. A. conceived the study. F. A. performed the synthesis with help from T. G. F. A. conducted all the characterizations and data analysis. F. A. and S. S. wrote the manuscript.

This research was supported by the NSF under Award No. DMR 2048285. F. A. acknowledges the funding support from the United Arab Emirates University under the National Faculty Support Program. We acknowledge Rachel Behrens and Cesar Rodriguez for assistance with the GPC and Hootan Roshandel for assistance with the DOSY spectroscopy. The MRL Shared Experimental Facilities at UCSB are supported by the MRSEC Program of the NSF under Award No. DMR 2308708. NEO 600 is supported by the S10 program of the NIH Office of Research Infrastructure Programs under grant S10OD028644.

Data availability

The data supporting this article have been included as part of the ESI.†

Conflicts of interest

The authors declare the following potential conflict of interest: a provisional patent application related to the content of this manuscript has been filed.

Notes and references

1 J. W. Yang, R. B. Bai, B. H. Chen and Z. G. Suo, *Adv. Funct. Mater.*, 2020, **30**, 1901693.
2 B. P. Lee, P. B. Messersmith, J. N. Israelachvili and J. H. Waite, *Annu. Rev. Mater. Res.*, 2011, **41**, 99–132.
3 B. K. Ahn, *J. Am. Chem. Soc.*, 2017, **139**, 10166–10171.
4 J. H. Waite, *Int. J. Adhes. Adhes.*, 1987, **7**, 9–14.
5 B. P. Lee, J. L. Dalsin and P. B. Messersmith, *Biomacromolecules*, 2002, **3**, 1038–1047.
6 Q. Zhao, D. W. Lee, B. K. Ahn, S. Seo, Y. Kaufman, J. N. Israelachvili and J. H. Waite, *Nat. Mater.*, 2016, **15**, 407–412.
7 J. Yang, V. Saggiomo, A. H. Velders, M. A. Cohen Stuart and M. Kamperman, *PLoS One*, 2016, **11**, e0166490.
8 M. Guvendiren, D. A. Brass, P. B. Messersmith and K. R. Shull, *J. Adhes.*, 2009, **85**, 631–645.
9 M. Yu and T. J. Deming, *Macromolecules*, 1998, **31**, 4739–4745.
10 B. P. Lee, C.-Y. Chao, F. N. Nunalee, E. Motan, K. R. Shull and P. B. Messersmith, *Macromolecules*, 2006, **39**, 1740–1748.
11 J. L. Dalsin, L. Lin, S. Tosatti, J. Voros, M. Textor and P. B. Messersmith, *Langmuir*, 2005, **21**, 640–646.
12 H. Montazerian, A. Hassani Najafabadi, E. Davoodi, R. Seyedmahmoud, R. Haghniaz, A. Baidya, W. Gao, N. Annabi, A. Khademhosseini and P. S. Weiss, *Adv. Healthcare Mater.*, 2023, **12**, e2203404.
13 J. Wang, C. Liu, X. Lu and M. Yin, *Biomaterials*, 2007, **28**, 3456–3468.
14 L. Li, Y. Li, X. Luo, J. Deng and W. Yang, *React. Funct. Polym.*, 2010, **70**, 938–943.
15 X. T. Wang, X. Deng, T. D. Zhang, J. Zhang, L. L. Chen, Y. F. Wang, X. Cao, Y. Z. Zhang, X. Zheng and D. C. Yin, *ACS Macro Lett.*, 2022, **11**, 805–812.
16 M. Cencer, Y. Liu, A. Winter, M. Murley, H. Meng and B. P. Lee, *Biomacromolecules*, 2014, **15**, 2861–2869.
17 K. M. Mattson, A. A. Latimer, A. J. McGrath, N. A. Lynd, P. Lundberg, Z. M. Hudson and C. J. Hawker, *J. Polym. Sci., Part A: Polym. Chem.*, 2015, **53**, 2685–2692.
18 E. Shin, C. Lim, U. J. Kang, M. Kim, J. Park, D. Kim, W. Choi, J. Hong, C. Baig, D. W. Lee and B.-S. Kim, *Macromolecules*, 2020, **53**, 3551–3562.
19 K. Olofsson, V. Granskog, Y. Cai, A. Hult and M. Malkoch, *RSC Adv.*, 2016, **6**, 26398–26405.
20 N. Illy and E. Mongkhoun, *Polym. Chem.*, 2022, **13**, 4592–4614.
21 N. B. Cramer, T. Davies, A. K. O'Brien and C. N. Bowman, *Macromolecules*, 2003, **36**, 4631–4636.
22 T. M. Roper, C. A. Guymon, E. S. Jönsson and C. E. Hoyle, *J. Polym. Sci., Part A: Polym. Chem.*, 2004, **42**, 6283–6298.
23 C. E. Hoyle and C. N. Bowman, *Angew. Chem., Int. Ed.*, 2010, **49**, 1540–1573.